01 Sep 2020

A Data-driven Approach For Predicting Nepheline Crystallization In High-level Waste Glasses

Irmak Sargin

Charmayne E. Lonergan
Missouri University of Science and Technology, clonergan@mst.edu

John D. Vienna

John S. McCloy

et. al. For a complete list of authors, see https://scholarsmine.mst.edu/matsci_eng_facwork/3222

Recommended Citation

I. Sargin et al., "A Data-driven Approach For Predicting Nepheline Crystallization In High-level Waste Glasses," *Journal of the American Ceramic Society*, vol. 103, no. 9, pp. 4913 - 4924, Wiley, Sep 2020. The definitive version is available at https://doi.org/10.1111/jace.17122

Received: 11 December 2019 | Revised: 14 March 2020 | Accepted: 18 March 2020

DOI: 10.1111/jace.17122

ORIGINAL ARTICLE

Journal of the American Ceramic Society

A data-driven approach for predicting nepheline crystallization in high-level waste glasses

Irmak Sargin[1] | **Charmayne E. Lonergan**[2] | **John D. Vienna**[2] | **John S. McCloy**[1,2] | **Scott P. Beckman**[1]

[1]School of Mechanical and Materials Engineering, Washington State University, Pullman, WA, USA

[2]Pacific Northwest National Laboratory, Richland, WA, USA

Correspondence
Scott P. Beckman, School of Mechanical and Materials Engineering, Washington State University, Pullman, WA 99 164, USA.
Email: scott.beckman@wsu.edu

Funding information
Nuclear Energy University Programs, Grant/Award Number: DE-NE0008597; U.S. Department of Energy, Grant/Award Number: 89304017CEM000001 and DE-AC05-76RL01830

Abstract

High-level waste (HLW) glasses with high alumina content are prone to nepheline crystallization during the slow canister cooling that is experienced during large-scale production. Because of its detrimental effects on glass durability, nepheline ($NaAlSiO_4$) precipitation must be avoided; however, developing robust, predictive models for nepheline crystallization behavior in compositionally complex HLW glasses is difficult. Using overly conservative constraints to predict nepheline formation can limit the waste loading to lower than the achievable capacity. In this study, a robust data-driven model using five compositional features has been developed to predict nepheline formation. A new descriptor is introduced called the "difference based on correlation", which has higher accuracy compared to previous descriptors and also has more balanced false positive and false negative rates. The analysis of the model and the data show an overlap, instead of a distinct compositional boundary, between glasses that form and do not form nepheline. As a result, the model's predictive accuracy is not the same throughout the feature space and instead is dependent on the location of the glass composition in the dimensionally reduced feature space.

KEYWORDS

data-science, classification, high-level waste glass, nepheline

1 | INTRODUCTION

Nuclear waste glasses are exceptional examples of highly complex multicomponent glasses; for example, typical waste glasses have >40 chemical components, as shown in the appendix to Vienna et al.[1] The high-level waste (HLW) glasses with high contents of Al_2O_3[2] and transition metals[3,4] are susceptible to devitrification. Wastes simultaneously rich in both Al_2O_3 and Na_2O tend to precipitate nepheline ($NaAlSiO_4$) during the slow cooling rates experienced in the center of the storage canister, that is, canister-centerline cooling (CCC) conditions,[5,6] whereas reactions among transition metal cations, primarily Fe, Cr, and Ni, cause spinel ($NiFe_2O_4$) formation.[2,3,7] While spinel crystallization may be problematic if it takes place inside the melter by reducing melter lifetime and performance,[4] nepheline is detrimental to waste form product performance due to the potential for poor aqueous chemical durability of the residual glass composition.[8,9] The overarching goal of waste form production is to immobilize the radionuclides and hazardous components from the environment for thousands to millions of years. The process of immobilizing radioactive tank waste will proceed more quickly, thereby reducing risk and cost, if the loading of waste is increased while maintaining adequate chemical durability.[10-12] Maximizing the loading of high-Al_2O_3 wastes is possible with higher Al_2O_3 and lower SiO_2 concentrations; however, this increases the tendency toward nepheline formation. Adding more SiO_2 prevents crystallization, ensuring

long-term environmental stability, but at the price of lowering the achievable waste loading.[13,14]

As a crystallization phenomenon, nepheline formation depends on thermodynamic and kinetic factors.[7,15-17] Technical efforts have focused on avoiding glass compositions that are prone to nepheline formation through the determination of the individual and collective effects of the initial glass components on nepheline precipitation.

1.1 | Compositional effect studies

Multi-component sodium aluminoborosilicate glasses are prone to nepheline precipitation and this tendency has been identified by a submixture rule that shows that nepheline forms if the Al_2O_3-Na_2O-SiO_2 submixture composition falls inside the nepheline primary phase field in the Al_2O_3-Na_2O-SiO_2 ternary phase diagram.[5,13] The effects of different elements on nepheline precipitation are not the same. First, Al_2O_3 is the most effective for inducing nepheline formation, followed by Na_2O and Li_2O.[5] The components Li_2O, K_2O, and Fe_2O_3 are equally effective. The least effective ones are CaO and SiO_2; the effect of SiO_2 is the opposite of others; instead of promoting, it inhibits nepheline formation.[5] Both the presence of B_2O_3 and the absence of Li_2O suppress nepheline precipitation.[6,13,18,19] Also, B_2O_3 is more impactful than SiO_2 at reducing the tendency for nepheline formation.[20] In nepheline-based glass-ceramic systems, boron stabilizes the residual glassy phase by increasing the tetrahedral boron (BO_4) unit concentration; boron stays in the glass and does not enter typical aluminosilicate crystal structures in the nuclear waste glass systems.[21-23] The effect of CaO on crystallization depends on whether it substitutes for Na_2O in the glass batch. If CaO replaces Na_2O, it suppresses nepheline formation, but if CaO is added to the glass composition without reducing the Na_2O amount, it promotes nepheline formation.[13,24,25] However, in the literature, contradicting reports are also present. Deshkar et al[26] examined the impact of varying CaO for Na_2O and SiO_2 in very simplified glass systems. They did not observe that CaO inhibits nepheline formation when replacing Na_2O, but instead reported that increasing the CaO/SiO_2 ratio induces the formation of cubic carnegieite, a mineral with the same nominal composition as nepheline but a different structure.

Acmite/aegirine ($NaFe_2SiO_6$) and nepheline form a solid solution,[27] therefore Fe may promote the formation of nepheline.[28] A study focusing on the effects of Fe-Al substitution shows that the effects of Fe additions on the solubility depends on the degree of this substitution.[27] Adding small amounts of Fe increases the nepheline formation tendency since Fe can be doped into Al sites in the nepheline structure. The substitution of Fe_2O_3 for Al_2O_3 or Na_2O in the initial glass composition lowers the onset temperature of crystallization, which is attributed to the prenucleation of iron oxide, creating a lower energy pathway for crystallization.[26] However, the excessive substitution of Fe for Al suppresses the formation of nepheline because there is insufficient Al.[27] Although Fe_2O_3 changes the mechanism and kinetics, its effect is relatively insignificant when high levels of boron are present, such as in aluminoborosilicate glasses.[26]

1.2 | Thermochemical, liquidus, and kinetic modeling approaches

Crystallization in nuclear waste glasses has been investigated by thermochemical means through the development of liquidus and/or crystallization models based on binary, ternary, or pseudoternary phase equilibria.[17,29] These thermochemical representation models mostly use an associate species[30-32] in which waste glass melts are represented by ideal solutions of simple 1-, 2-, and 3-component metal oxide melts.[33] Although there also exist quasichemical models,[34-36] the associate species model is more widely preferred due to its ease of application.[31,32]

The Na_2O-Al_2O_3-B_2O_3-SiO_2 system has been studied with the associated species model and it has been shown that the addition of SiO_2 and B_2O_3 can eliminate nepheline formation even within the nepheline primary phase field by decreasing the activity of Na_2O in the melt phase.[31] Also, the liquidus temperatures have been calculated, and lowering the nepheline formation temperature is identified as a potential means to avoid nepheline crystallization.[31] Similar studies have been conducted for Na_2O-Al_2O_3-SiO_2 and Na_2O-B_2O_3-SiO_2 systems.[30] These confirm the effect of B_2O_3 on the activity of Na_2O and also show that the addition of SiO_2 increases the activity of B_2O_3 in the cases where SiO_2 does not substitute for B_2O_3 in the glass melt; however, for situations where SiO_2 substitutes for B_2O_3, the addition of SiO_2 decreases the activity.[30] Another study on the Na_2O-Al_2O_3-B_2O_3-SiO_2 system showed that the liquidus temperatures vary irregularly with composition, although both Al_2O_3 and SiO_2 increase the liquidus temperature.[32]

In addition to these, a pseudobinary phase diagram between a transition metal ferrite spinel and nepheline has been defined using a quasicrystalline approach.[2,7] In this method, spinel and nepheline precursors are defined, and their interactions examined. The thermodynamical octahedral site preferences are found to govern the exchange equilibria between the quasicrystalline species in the melt and the crystalline species at the liquidus.

There also have been experimental studies in which the liquidus temperatures of different glasses have been measured and an empirical model has been fit to interpolate the liquidus temperatures of intermediate compositions.[37] Although the fits are generally non-linear, strong linear trends between

component concentrations and liquidus temperatures have been observed for the nepheline phase field.[6] It is found that Al_2O_3, B_2O_3, Na_2O, and SiO_2 are the main components affecting the liquidus temperature; a relationship between the Raman band corresponding to Al_{iv}-O-Si units and liquidus temperature was identified.[6]

Above the liquidus, structural elements of nepheline can exist,[38] allowing nepheline to precipitate rapidly when the temperature dips below the liquidus. The crystal growth, or dissolution, is controlled by diffusion and can be expressed using a modified Kolmogorov-Mehl-Johnson-Avrami Equation[15]

$$\frac{C}{C_e} = 1 - \exp\left[\left(-\frac{t}{\tau}\right)^n\right]. \quad (1)$$

From the comparison of kinetic and equilibrium coefficients of nepheline and spinel crystallization in HLW, it is known that the concentration of nepheline can be more than ten times higher than spinel, although their temperature dependencies are similar.[15] Their concentrations increase gradually as temperature decreases; however, the nepheline crystal growth is more sensitive to temperature change.[15] Also, at certain temperatures, nepheline concentrations can reach equilibrium values in one minute.[15] It is concluded that "…nepheline precipitation is extremely rapid at least in some glasses, thus leaving little room for its control by fast cooling."[15]

1.3 | Constraint model approaches

A comprehensive approach to managing HLW glass involving all-encompassing models to predict regions within the compositional space where nepheline crystallization occurs has yet to be identified. To date five different models have been proposed.

The first is called *nepheline discriminator* (ND) and is based on the principle that nepheline does not form outside its primary phase field in the Na_2O-Al_2O_3-SiO_2 submixture system.[5] The ND is defined as the normalized SiO_2 concentration in the submixture system making the ND constraint that if $\frac{g_{SiO_2}}{\left(g_{SiO_2}+g_{Al_2O_2}+g_{Na_2O}\right)} \geq 0.62$, no nepheline is expected.[5]

Although this constraint successfully determines the glasses that will precipitate nepheline, there are many glasses with ND values <0.62 that do not form nepheline.[13] In this sense, the ND is overly conservative. Another downside of the ND is that it does not take into account the known effects of the many other components detailed above. As a result, a less conservative and a more comprehensive method for predicting nepheline precipitation is needed.

As a remedy, McCloy et al[13] proposed the use of *optical basicity* (OB) along with ND. The rationale behind the introduction of OB is that the basicity of the cations allows the prediction of their effects on aluminosilicate precipitation. Melts with OB < 0.575 are expected to have a lower tendency toward nepheline formation. Here, ND and OB are used together in a quadrant system based on threshold values. The OB is successful in explaining the effects of acidic oxides B_2O_3, SiO_2, and P_2O_5. Although OB has improved the shortcomings of ND, it is still conservative towards high-alumina wastes in glass.[14,18]

A *neural network* model was developed to incorporate the complex nonlinear interactions between components using 629 glasses.[1] The architecture of the neural network was a single layer with three nodes, of which the activation function was chosen as a hyperbolic tangent. The model predicted nepheline formation with a probability threshold of 0.27. The misclassification rate of the model was 8%. Although the model provides valuable insights about the effects of B_2O_3 and Li_2O, due to the "black box" nature of the neural network, physical interpretation of the components' effects and determination of uncertainties are difficult.

More recent models for predicting nepheline formation are based on a *submixture model* (SM)[20] that is an extended version of ND that includes the effects of the alkali and alkaline-earth oxides, B_2O_3, P_2O_5, and Fe_2O_3. A pseudoternary phase diagram is used with the alkali and alkaline earth oxides as the first component, $Al_2O_3 + Fe_2O_3$ as the second, and $SiO_2 + B_2O_3 + P_2O_5$ as the third. Two different approaches have been used. In the first, a polynomial curve, discriminating between the presence and absence of nepheline, was calculated after the glass compositions were projected on the pseudoternary system.[20] In the second, instead of a polynomial curve,[20] a logistic regression model was used to predict nepheline formation and instead of submixtures, dimensionally reduced components are used.[39] Both models were tested on the same dataset of 747 glass dataset. The polynomial had a misclassification rate of 8.3%, and the logistic regression model a misclassification rate of 8.2%. The predictive methods reviewed here are summarized in Table 1.

In this study, we use an extended version of the glass dataset from SM studies[20,39] and develop a *nonparametric, predictive* model for nepheline formation. We discover the existence of an "overlapping" region, that is, a region of composition space where samples with similar compositions exhibited different crystallization behavior, that limits the accuracy of the model. Most of the glasses misclassified by our model are in this overlapping region. We also propose a *dimensionality reduction* method to quantify the accuracy of the model's predictions as a function of composition.

2 | DATA AND METHOD

The data used in this study were also used for the submixture model developed by Vienna et al.[20] Of the 747 glass compositions taken from the literature, 90 of them were specifically

TABLE 1 Summary of previous classification schemes. The misclassification rate is given for the dataset with 747 glasses from Ref. [20]

Classification scheme	Misclassification rate	Limitations	Reference
Nepheline discriminator (ND)	36.1%	Overly conservative Does not consider the well-known effects of many of the components	[5]
Nepheline discriminator + optical basicity (ND + OB)	27.7%	Although recovered ND's over conservatism, still conservative	[13]
Artificial neural network (ANN)	8.0%	High accuracy difference between train and test set The quantification of uncertainties is difficult.	[1,20]
Submixture model with the polynomial fit (SM)	8.3%	Higher fractions of false negative than desired	[20]
Non-linear regression and dimensionally reduced components (NLR-DRC)	8.6%	According to the chosen threshold, either false positive or false negative rate is higher than acceptable values.	[39]

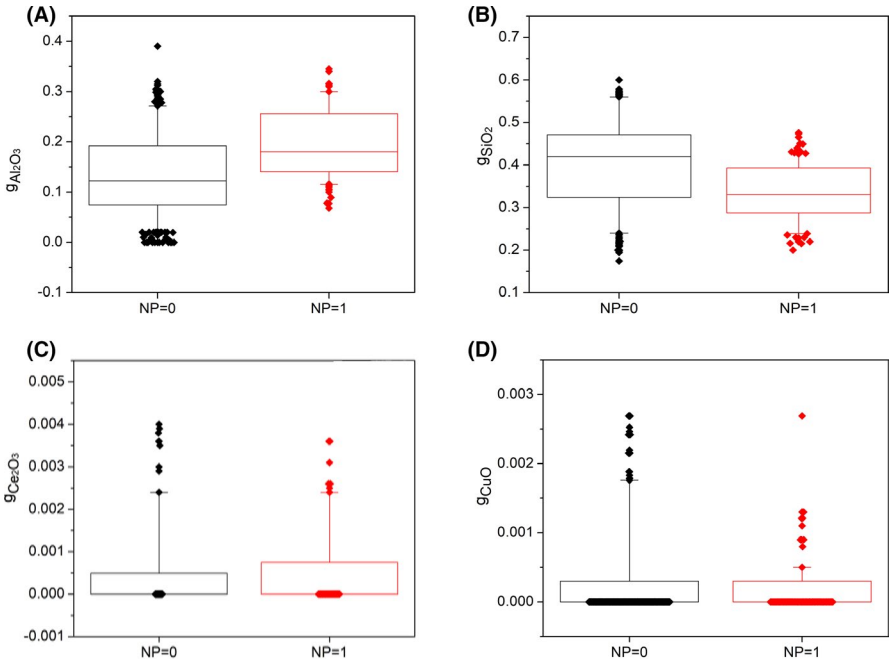

FIGURE 1 Different types of relationships between the target variable and the mass fractions, *g*, of the oxide in the glass including (A) strong positive association, (B) strong negative association, (C) implicit relationship, and (D) no distinguishable relationship. Box plots for all the components are given in Figure S1 [Color figure can be viewed at wileyonlinelibrary.com]

designed to examine the two- and three-component effects found in high-alumina HLW glasses. All glasses were simulated HLW compositions and were treated by several different CCC patterns. The details of the data are given elsewhere.[20,40,41] In addition to these, two glass matrices (NP5-01 through NP5-27 plus BL3 and NP6-01 through NP6-20) were used as validation sets. Both of these sets of glass compositions were designed by a space-filling design and details of the design, glass, and heat treatment conditions are given in references.[40-42]

2.1 | Informatics approach

Data analysis and classification studies have been conducted using the Scikit-learn package.[43] The data were first examined to understand if the content of a specific oxide was different in the nepheline-forming glasses than others. The analysis was visualized by the component concentration box plots as demonstrated in Figure 1. Box plots for all the components are given in Figure S1. Here, NP = 0 corresponds to the amount of the oxide distribution in the glasses that do not form nepheline, and NP = 1 shows glasses that do form nepheline. The upper and lower limit of the box shows the 25th and 75th percentiles, while the whiskers show the 95th and 5th percentiles, the horizontal line is the median, and diamond symbols are outliers, which are defined as those points outside the 5th and 95th percentiles.

It was observed that there were three different relationships between nepheline formation and oxide content. The first relationship involved a strong association between the nepheline formation and the amount of the oxide, meaning there was a significant difference between the median of the distribution in the two different classes (NP = 0 and NP = 1)

of glasses. The association was considered strong if the difference between medians was higher than 5%. The oxides showing this behavior were as follows: Al_2O_3, B_2O_3, BaO, Cr_2O_3, CdO, F, K_2O, La_2O_3, MgO, MnO, Na_2O, NiO, P_2O_5, PbO, SiO_2, TiO_2, ZnO, and ZrO_2. This relationship was either positive, indicating the oxide enhanced nepheline formation, as shown in Figure 1A for Al_2O_3, or negative, meaning the oxide hindered nepheline formation, as shown in Figure 1B for SiO_2.

A second relationship involved the oxides in which the median values did not demonstrate a strong association, but an implicit differentiation was inferred from the distribution width. A wider distribution indicates that the amount of oxide does not have a definite effect; in contrast, a narrower distribution implies that the amount of the oxide has a lower variation among the glasses in the same class. As shown in Figure 1C, the distribution of Ce_2O_3 in glasses that do not form nepheline was narrower than that of the ones that formed nepheline, suggesting that this oxide may have a suppressing effect. To characterize this association, the range of oxides after outliers were taken out was calculated for the oxides that have a median difference of <5%. If the range difference between nepheline forming and not forming glasses was higher than 10%, they were assumed to be in this group. The oxides that demonstrated this relationship were as follows: CaO, Ce_2O_3, CeO_2, Fe_2O_3, Li_2O, MoO_3, Nd_2O_3, PdO, SO_3, SrO.

The third possible relationship consisted of inconclusive oxides, due to their only being added in minimal amounts for a very limited number of glasses. An example is shown in Figure 1D.

After observing these relationships, a new descriptor was created that is the mass fraction difference between oxides that have positive associations with nepheline formation and those with negative associations. Different combinations of the parameters were tried to find the best. Details of the selection of this new descriptor are given in the discussion. This term is referred to as the "*difference based on correlation*" (DC) descriptor.

$$\begin{aligned} DC = (&g_{Al_2O_3} + g_{Cr_2O_3} + g_{P_2O_5} + g_{K_2O} \\ &+ g_{Na_2O} + g_{Li_2O} + g_{TiO_2}) - (g_{B_2O_3} + g_{Ce_2O_3} \\ &+ g_{La_2O_3} + g_{Nd_2O_3} + g_{CeO_2} + g_{SO_3} + g_{MoO_3} \\ &+ g_{CdO} + g_{PdO} + g_{NiO} + g_{SrO} + g_{ZrO_2}) \end{aligned} \quad (2)$$

The criterion for nepheline presence is DC ≥ 0.26.

Nepheline formation from HLW glass depends heavily on the thermal processing, although it is not yet known whether the different CCC cycles used in the studies impact the results. Therefore, heat-treatment-related features were included. Eight different parameters were extracted by digitizing the CCC profiles given in table 2 in Ref. [1] and citations therein: the duration in minutes residing between the temperature ranges ΔT = 1200-1050°C, ΔT = 1050-980°C, ΔT = 980-930°C, ΔT = 930-875°C, ΔT = 875-825°C, ΔT = 825-775°C, and ΔT = 775-725°C; the cooling rate in range defined by (highest-725)/time(°C/min.), and overall cooling rate (highest-lowest)/time(°C/min.).

3 | DATA ANALYSIS

The addition of heat-treatment-related parameters resulted in 60 attributes; the first step of the classification study was feature selection by recursive feature elimination (RFE). This feature selection method was preferred because it uses models that allow the contributions of features to be observed, allowing scientific understanding. The classification algorithms evaluated were support vector machines, random forests, decision trees, and decision trees with adaptive boosting (AdaBoost). Among these, the most successful was decision trees with AdaBoost. AdaBoost combines multiple weaker learners, which are decision trees with a single split, called decision stumps, and turns them into a single strong learner. To make a strong learner out of weak ones, AdaBoost assigns more weight to the samples that are difficult to classify and less weight to the ones already easily predicted. The accuracy, that is, the ratio of true predictions to all predictions, was used as the quality metric and five features were identified: CaO, Na_2O, DC, ND, and OB. Other quality metrics also were tested including the precision, the ratio of true positives to sum of true positives and false positives, the recall, the ratio of true positives to sum of true positives and false negatives, and finally the F1 score, the harmonic mean of precision and recall. Although using different quality metrics identified different features, the overall performance of the model did not improve, which was the goal of this activity. The software written for this study is included in the Supplementary Materials.

To ensure that every sample in the dataset had the chance of appearing in both training and test sets, five-fold cross-validation was used while determining the parameters of the model. During cross-validation, care was taken to ensure that the same relative amount of nepheline-forming and non-nepheline-forming glasses were used in the splits. Random sampling could not be used because there was a class imbalance in the dataset; only 28% of the 747 samples were nepheline-forming glasses.

The stability of the model was verified using 1000 training-test sets, again sampled to have the correct amount of nepheline-forming and non-nepheline-forming glasses. The model was trained and then tested over 1000 different subsets of the original dataset, and the results are given in Figure 2. The maximum accuracy, precision, and recall were 0.957, 0.977, and 0.981, respectively, the minimum values were 0.850, 0.686, and 0.692, and the mean values were 0.913, 0.837, and 0.856. We are reporting the precision and recall values along with accuracy because they provide insight into

the model beyond its predictive power. The precision shows the relative conservatism of the model; as it increases, the model becomes less conservative, meaning that compositions with higher loading are less likely to be eliminated. The precision was 0.43 for the ND model and 0.50 for the ND + OB one, making the new model, with precision of 0.70 significantly less conservative than either of these. The recall shows the relative capacity for discriminating between the classes; as it increases the number of false negatives decreases improving the overall capability of the model.

Although it is not possible to simultaneously increase the precision and recall, the model developed here provided a compromise between the two. The numbers of false negative and false positive identifications averaged over 1000 different test sets, were 7.500 and 8.803, respectively, in the 187 glasses. This distribution suggests that the model was not equally successful throughout all of the feature space. The most frequently misclassified glasses in the 1000 different test sets were identified to determine the regions where the model was less accurate. Of the 747 glasses, only 71 were misclassified as false negatives and 72 as false positives. The ones that were misclassified greater than 50% of the time were identified, and it was found that there were 28 false negatives and 35 false positives.

Since only a small percentage of the samples were frequently misclassified, the leave-one-out (LOO) method was used to determine the extent that these particular samples fit outside the predictive capacity of the model. In this method, one data point at a time forms a test set, and the rest of the dataset is used for training.

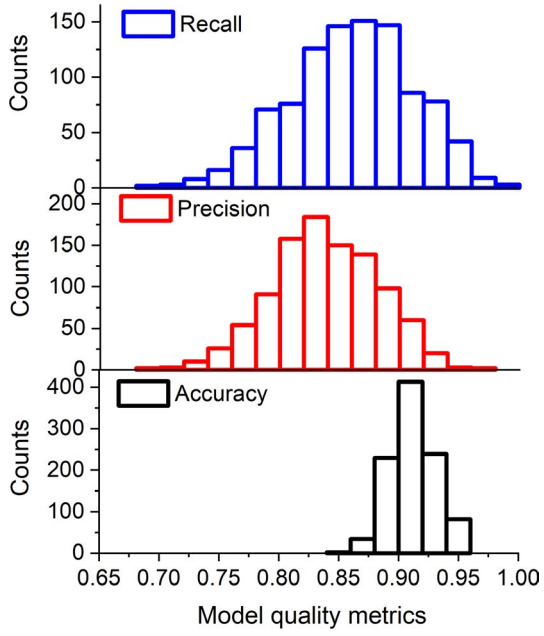

FIGURE 2 Distribution of accuracy, precision, and recall of the 1000 different test sets [Color figure can be viewed at wileyonlinelibrary.com]

The resulting accuracy was 0.921, precision was 0.852, and recall was 0.865, with 31 false positives and 28 false negatives. The 59 misclassified glasses were compared to those previously identified, and it was found that all 35 of the false positives agreed and 24 of the 28 false negatives agreed.

The values of the misidentified glasses were compared to the full dataset to determine if there were specific feature ranges where misclassification occurred; Figure 3 demonstrates that this was indeed the case. Unfortunately, those ranges also coincided with the highest populated range in all the datasets; therefore, the misclassification could not be explained simply by individual features.

These results suggest that, at least for a select range of the feature set, the classes overlap within this range; that is, glasses with very similar features belong to opposing classifications. Dimensionality reduction, in the form of principal component (PC) analysis, was applied to verify this hypothesis and identify the regions of feature space where it existed. Figure 4A shows the first two PC results, reduced from the five features identified above, CaO, Na_2O, DC, ND, and OB. Most of the misidentified glasses resided on or near the hypersurface between the glass compositions that formed nepheline and those that did not. Several false positives did not form nepheline although they were in the nepheline-forming region. To determine if the existence of overlapping classes is unique to the selected feature set, dimensionality reduction was also applied to the dataset containing all features. As shown in Figure 4B, when all features were used, it was almost impossible to differentiate class regions. The PC analysis of the selected feature subspace has the potential to be more useful for distinguishing between classes than analysis using the entire feature space. Also, this observation validates the five features selected to represent the data.

The principal component space was divided into four zones to determine the ranges in PC space where the overlapping occurs. The zones were characterized in terms of percentage of nepheline forming glasses (%NPG), model accuracy, percentage of false negatives, and percentage of false negatives in that zone. These are given in Table 2. Using these zones allows for estimating the variation of accuracy as a function of composition. The software used for dimensionality reduction and determination of zones is provided in Supplementary Materials.

We have applied the model to examine the Pacific Northwest National Laboratory Phase 5 (NP5-) and Phase 6 (NP6-) glass compositions. These glass compositions were selected based on previous models[40,41] to be in the compositional region with the most uncertainty and, in agreement with expectations, most of these samples fell within the overlapping regions in PC space, Zone 2 and Zone 3, as expressed in Table 3. The commonly misclassified glasses were not included in the training set because

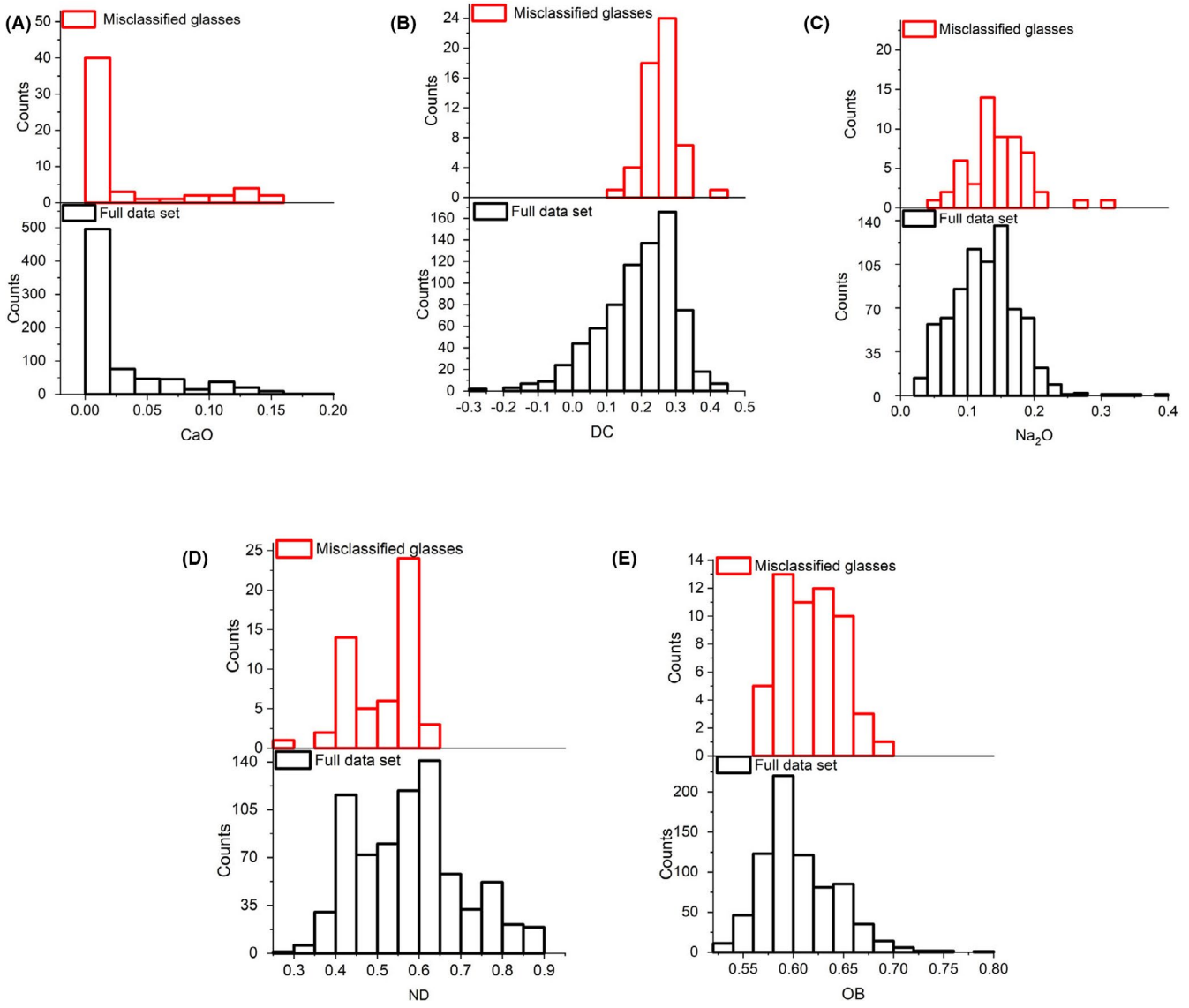

FIGURE 3 Distribution of the selected features allowing comparison between misclassified and full dataset for the five features used in the classification model [Color figure can be viewed at wileyonlinelibrary.com]

FIGURE 4 Visualization of the data in principal component space that is dimensionally reduced from (A) selected feature space and (B) all 60 features [Color figure can be viewed at wileyonlinelibrary.com]

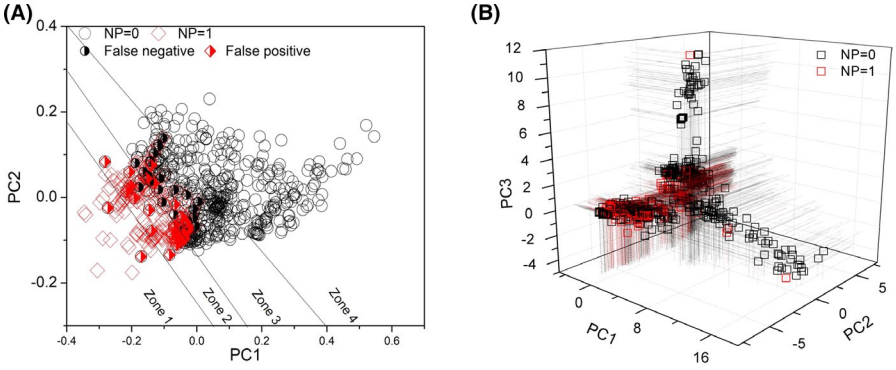

they decreased the accuracy of the predictions. The accuracy of the model for these samples was 80% with five false negatives and five false positives among 48 samples, of which 35% precipitated nepheline. All of the misclassified glasses were in PC Zone 2 and Zone 3.

4 | DISCUSSION

An important outcome of this study is the introduction of the new single descriptor DC that can be used alone for prediction of nepheline formation. To compose this

TABLE 2 Zones in the DC space, percentage of nepheline forming glasses, percentage of true predictions, percentage of false negatives, and percentage of free negatives

Zone#	%NPG	%True prediction	% False positive	% False negative
1	96%	96%	4%	0%
2	74.8%	83.5%	15.7%	0.8%
3	20.8%	90.1%	2.9%	7.0%
4	0%	100%	0%	0%

parameter, we tried different combinations of the strongly and implicitly associated oxides. In an extreme case, all the oxides with strong and implicit association from the dataset were included in the parameter. This trial resulted in an accuracy of 0.795 with 76 false negatives and 76 false positives. Another extreme approach involved only using only the oxides known to dominate the waste stream: Al_2O_3, Na_2O, P_2O_5, B_2O_3, SiO_2, and Fe_2O_3. This approach resulted in an accuracy of 0.798 with 50 false positives and 101 false negatives. The large difference between number of false negatives and false positives shows that this parameter suffers from class imbalance. The highest accuracy, with a well-balanced false negative and false positive rate, is provided by the combination presented as DC in Equation (2) above.

Although the absence of some oxides can be associated with the fact that their amounts are very small, it is surprising that the oxides with known effects such as SiO_2, Fe_2O_3, and CaO, decrease the accuracy of this descriptor. This surprising effect is probably purely data-driven and due to the fact that DC is a linear sum. For CaO and Fe_2O_3, their effects cannot be clearly deduced from the distribution plots. There are other oxides with similar trends that do not decrease the accuracy of DC, indicating that the effect of CaO and Fe_2O_3 are dependent on the amounts of other oxides. This agrees with the findings in the literature. On the other hand, the decrease in accuracy with the addition of SiO_2 is related to its relatively higher values in the glass batches. From an entirely mathematical point of view, when the amount of SiO_2 is used in the linear sum, it may be masking the more subtle effects provided by the less prevalent oxides.

Table 4 shows a comparison of three different descriptors: ND, ND + OB, and DC in the form of a confusion matrix, which visualizes the performance of a classifier in terms of the number of true positives (TP), true negatives (TN), false positives (FP), and false negatives (FN). The columns are the actual classes and rows are the predicted classes. The ND estimates all nepheline formers correctly and any misidentified glass is a false positive. This outcome demonstrates the conservative nature of ND. A similar situation also is observed for ND + OB; most of the misidentified glasses are false positives.

By contrast, DC has a ratio of false negatives to false positives of 0.8. The difference in the number of false negatives for ND, ND + OB, and DC demonstrates that DC is a less-conservative discriminator, while at the same time, its accuracy for this dataset (84%) is higher than ND and ND + OB. We present DC, not as a standalone model, but instead we present it as the first attempt to develop a data-driven single descriptor. There is room for improvement, and because it is a linear sum of oxide contents in the glass melt, this task may be relatively easy. One approach to enhance DC may involve the addition of linear scaling coefficients to each term in the expansion. The value of these coefficients could be adjusted via regression until DC is optimized for the particular glass data.

Incorporating the new DC parameter and applying the feature elimination algorithm allows the development of a model, with an overall accuracy of 92.1%, comprised of only five features that are successful over a substantial compositional region. Most of the misprediction stemmed from the subregion of feature space that is the hypersurface between the regions of glasses forming or not-forming nepheline. The PC analysis allows accurate identification of this intersection region. The zone boundaries are selected so that nepheline-forming glasses primarily occupy Zone 1. Zone 2 is mainly nepheline-forming glasses and false positives with only one false negative. This zone is the overlapping region on the nepheline forming side. Zone 3 is the overlapping region on the non-nepheline-forming side. All false negatives, except a single one in Zone 2, are in Zone 3. Although there are some false positives, their number is relatively low in comparison to the false negatives. Finally, Zone 4 only has non-nepheline-forming glasses. The difference in the number of false positives and false negatives between the four zones explain the higher variation of the precision and recall in comparison to accuracy, as shown in Figure 2.

Among the glasses in Zone 1, only two do not form nepheline, and these are the only misclassified ones. The presence of these two glasses may be explained by the presence of other crystals than nepheline.[24] The accuracy of Zone 4 is 100%. In Zone 2 the risk of predicting a false positive is greater a false negative, and a reverse is true for Zone 3.

The distribution of values of all compositional and heat treatment-related features in all zones are examined for both true and false predictions; no significant difference is observed. Within each zone, the distribution of values for each feature is nearly the same.

No evidence yet exists to explain the overlapping regions. Potential hypotheses for its existence fall into two categories, physics based and data based. Physics-based hypotheses focus on the sensitivity of some glasses to small changes in composition, cooling rate, homogenization, and other processing factors. These variations may be within the limits of experimental precision but still lead

TABLE 3 Glass ID, PC zone, nepheline formation, and model prediction of the test set

Glass ID	PC zone	Nepheline formation	Prediction
NP5-01	3	No	True
NP5-02	3	No	True
NP5-03	4	No	True
NP5-04	3	No	True
NP5-05	2	Yes	False negative
NP5-06	4	No	True
NP5-07	3	No	True
NP5-08	2	No	False positive
NP5-09	3	No	False positive
NP5-10	2	No	False positive
NP5-11	3	Yes	True
NP5-12	3	No	True
NP5-13	3	Yes	True
NP5-14	3	No	True
NP5-15	3	No	True
NP5-16	1	Yes	True
NP5-17	4	No	True
NP5-18	3	No	True
NP5-19	3	Yes	True
NP5-20	3	No	True
NP5-21	2	Yes	True
NP5-22	3	No	True
NP5-23	3	Yes	True
NP5-24	3	Yes	True
NP5-25	1	Yes	True
NP5-26	3	No	True
NP5-27	3	Yes	True
BL3	2	Yes	True
NP6-01	3	No	True
NP6-02	3	No	True
NP6-03	2	No	True
NP6-04	3	Yes	False negative
NP6-05	3	No	True
NP6-06	2	No	True
NP6-07	3	Yes	False negative
NP6-08	3	Yes	False negative
NP6-09	2	No	False positive
NP6-10	3	Yes	True
NP6-11	3	No	False positive
NP6-12	3	No	True
NP6-13	3	No	True
NP6-14	3	No	True
NP6-15	3	No	True
NP6-16	3	No	True
NP6-17	3	No	True
NP6-18	3	No	True
NP6-19	3	Yes	False negative
NP6-20	3	Yes	True

to significantly different results. This hypothesis requires the free energy for nucleation to be relatively small, within the fluctuations in the overlapping region. To resolve this issue, more complex features involving interactions may be required. Although the CCC features are not prevalent in the current classification model, their interaction with compositional parameters may be important in the overlapping regions, Zones 2 and 3. The reason such interactions are not selected by the feature elimination methods used here may be their being low importance for the data in Zones 1 and 4. To address this, classification models including only the overlapping region must be developed. The data-based hypotheses focus on sampling within the overlap region and the possible absence of sufficient number of examples. Increasing the number of samples may facilitate the development of better features to allow distinction between the competing classes.

Two different feature importances, plotted in Figure 5, are considered to understand the decision of the model. The feature importances of tree-based models are the percentage of the samples for which the selected feature plays a major role in the decision. For AdaBoost, the feature importance is a weighted average of the samples where the selected features play a major role. The feature importance is a weighted average for the AdaBoost because AdaBoost gives higher weight to the difficult-to-predict samples. This is shown in Figure 5A. We can say that for the samples in Zone 2 and Zone 3 the decision is driven most frequently by the amount of Na_2O followed by DC, ND, OB, and CaO. The overall feature importances are presented by permutation importances. Permutation feature importances are calculated by assigning a constant value for the selected features of all samples and then measuring the accuracy of the model. This analysis shows the largest decrease in accuracy is a result of the elimination of ND, and the smallest is a result of the elimination of CaO.

The previous models, ANN,[1] SM,[20] NLR-DRC,[39] and this model all have very similar accuracies, around 92%. The model presented here is more balanced in terms of rate of false negatives, 28 out of 212 or 13.2%, and false positives, 35 out of 535 or 6.5%, and both of these rates are within acceptable limits.[20,39] On the other hand, the SM model has a false negative rate that is higher than the desirable.[20] For the

	Actual class					
Predicted class	**Positive**			**Negative**		
Positive	ND	ND + OB	DC	ND	ND + OB	DC
	206	192	161	273	206	67
Negative	ND	ND + OB	DC	ND	ND + OB	DC
	0	14	53	268	335	473

TABLE 4 Confusion matrix for ND, ND + OB, and DC. The upper left quadrant is TP, and proceeding clockwise the quadrants are FP, TN, and FN

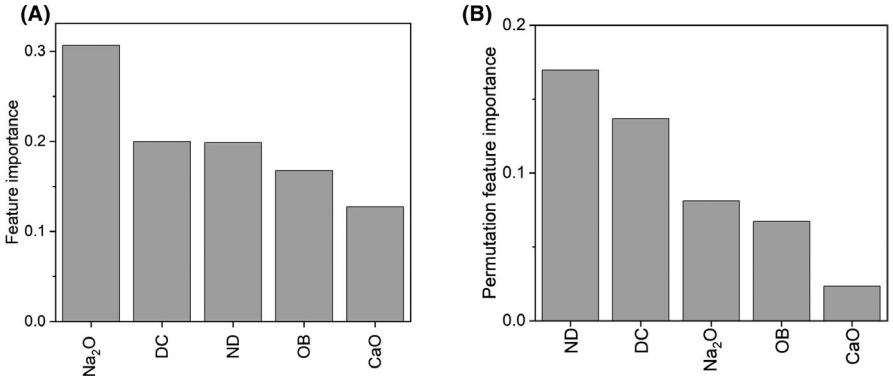

FIGURE 5 Feature importances as obtained from (A) boosted decision trees, (B) permutation importances method

NLR-DRC model, depending on the threshold value used, either false positive or false negative rates are too high.[39] The maximum Al_2O_3 concentration allowed prior to predicting nepheline formation by our model is 32 wt.%, whereas the maximum Al_2O_3 concentration allowed when the decision is based on ANN model is 28.24 wt.%, which was the highest allowed until the present study.[20] Also, the model presented here provides an analysis of model reliability and false prediction character; that is, if there is a wrong prediction, which kind, false negative or false positive, is the greater probability, based on the sample's position in the feature space.

The similarity between the accuracy of the previous models and this model suggests that the predictive power of previous models is also limited by the existence of the overlap region. Test samples (NP5- and NP6-) show that the overlapping regions include the glasses with high alumina content. Without further analysis of the overlapping region, it will not be possible to develop a model with uniformly high accuracy across the entire design space. In particular, the regions of most significant interest, samples with alumina content that can take high loading of waste products, remain uncertain.

5 | SUMMARY AND CONCLUSIONS

A new data-driven descriptor for the prediction of nepheline formation in HLW glass is introduced, which is a linear combination of the oxide compositions. Using this and four additional composition-derived features, a robust data-driven model, with 92.1% accuracy, is developed to predict nepheline formation. The most important feature for differentiating between glasses that form nepheline and those that do not in the "overlapping regions" (Zone 2 and Zone 3) is the Na_2O content, whereas for the overall dataset, ND and DC are the most important features. Additionally, the accuracy of the model depends on the location within the reduced feature space. Examination of the reduced feature space provides insight on the accuracy and uncertainty of the model; it is determined that there exists an intersection between the classes of glasses that did or did not form nepheline. Additional work is required to understand the existence of this overlap region, but several hypotheses have been identified.

ACKNOWLEDGMENTS

This research was performed using funding received from the US Department of Energy (DOE) Offices of Nuclear Energy and Environmental Management through the Nuclear Energy University Program under the award DE-NE0008597, and the Office of River Protection (ORP) award number 89304017CEM000001. The PNNL authors acknowledge generous support from the DOE-ORP Waste Treatment Plant Program Office. This work was overseen by Dr. Albert Kruger (DOE-ORP) who supplied valuable guidance and direction. Pacific Northwest National Laboratory is operated by Battelle Memorial Institute for the DOE under contract DE-AC05-76RL01830.

ORCID

Irmak Sargin https://orcid.org/0000-0001-5156-5448
Charmayne E. Lonergan https://orcid.org/0000-0003-2667-4815
John S. McCloy https://orcid.org/0000-0001-7476-7771
Scott P. Beckman https://orcid.org/0000-0002-8156-6684

REFERENCES

1. Vienna JD, Skorski DC, Kim DS, Glass MJ. Property models and constraints for estimating the glass to be produced at Hanford by implementing current advanced glass formulation efforts. Richland, WA: Pacific Northwest National Laboratory; 2013. Report No.: PNNL-22631.
2. Jantzen CM, Brown KG. Predicting the spinel-nepheline liquidus for application to nuclear waste glass processing. Part I: primary phase analysis, liquidus measurment, and quasicrystalline approach. J Amer Ceram Soc. 2007;90(6):1866–79.
3. Hrma P, Riley BJ, Crum JV, Matyas J. The effect of high-level waste glass composition on spinel liquidus temperature. J Non-Cryst Solids. 2014;384:32–40.
4. Matyas J, Vienna J, Kimura A, Schaible M, Tate R. Development of crystal-tolerant waste glasses. 2010;222:41–50.
5. Li H, Vienna JD, Hrma P, Smith DE, Schweiger MJ. Nepheline precipitation in high-level waste glasses: compositional effects and impact on the waste form acceptability. In: Gray WJ, Triay IR, editors. Proceedings of MRS. 465, Scientific Basis for Nuclear Waste Management XX. Pittsburgh, PA: Materials Research Society, 1997; p. 261–8.
6. Li H, Hrma P, Vienna JD, Qian M, Su Y, Smith DE. Effects of Al_2O_3, B_2O_3, Na_2O, and SiO_2 on nepheline formation in borosilicate glasses: chemical and physical correlations. J Non-Cryst Solids. 2003;331(1–3):202–16.
7. Jantzen CM, Brown KG. Predicting the spinel-nepheline liquidus for application to nuclear waste glass processing. Part II: quasicrystalline freezing point depression model. J Amer Ceram Soc. 2007;90(6):1880–91.
8. Riley BJ, Hrma P, Rosario J, Vienna JD. Effect of crystallization on high-level waste glass corrosion. In: Smith GL, Sundaram SK, Spearing DR, editors. Ceramic transactions. Westerville, OH: The American Ceramic Society, 2001; p. 257–65.
9. Kim DS, Peeler DK, Hrma P. Effect of crystallization on the chemical durability of simulated nuclear waste glasses. In: Jain V, Palmer R, editors. Ceramic transactions. Westerville, OH: American Ceramic Society, 1995; p. 177–85.
10. Jantzen CM, Cozzi AD, Bibler NE. High level waste processing experience with increased waste loadings. In: Vienna J, Herman C, Marra S, editors. Ceramic transactions. Westerville, OH: American Ceramic Society, 2004; p. 31–49.
11. Hrma P, Vienna JD, Schweiger MJ. Liquidus temperature limited waste loading maximization for vitrified HLW. In: Jain V, Peeler DK, editors. Ceramic transactions. Westerville, OH: American Ceramic Society, 1996. p. 449–56.
12. Vienna JD. Nuclear waste vitrification in the United States: recent developments and future options. Int J Appl Glass Sci. 2010;1(3):309–21.
13. McCloy JS, Schweiger MJ, Rodriguez CP, Vienna JD. Nepheline crystallization in nuclear waste glasses: progress toward acceptance of high-alumina formulations. Int J Appl Glass Sci. 2011;2(3):201–14.
14. Goel A, McCloy JS, Pokorny R, Kruger AA. Challenges with vitrification of Hanford high-level waste (HLW) to borosilicate glass – an overview. J Non-Cryst Solids. 2019;4:100033.
15. Menkhaus TJ, Hrma P, Li H. Kinetics of nepheline crystallization from high-level waste glass. In: Chandler GT, Feng X, editors. Ceramic transactions. Westerville, OH: American Ceramic Society, 2000; p. 461–8.
16. Amoroso J. The impact of kinetics on nepheline formation in nuclear waste glasses. Medium: ED. Aiken, SC: Savannah River National Laboratory; 2011. Report No.: SRNL-STI-2011-00051.
17. Utlak SA, Besmann TM. Thermodynamic assessment of the Na_2O-Al_2O_3-SiO_2-B_2O_3 pseudo-binary and -ternary systems. J Chem Thermodyn. 2019;130:251–68.
18. Kroll JO, Vienna JD, Schweiger MJ. Effects of Al_2O_3, B_2O_3, Li_2O, Na_2O, and SiO_2 on nepheline crystallization in hanford high level waste glasses. In: Ohji T, Kanakala R, Matyáš J, Manjooran NJ, Pickrell G, Wong-Ng W, editors. Ceramics transactions. Hoboken, NJ: John Wiley & Sons, Inc., 2016; p. 159–69.
19. Fox KM, Edwards TB, Peeler DK. Control of nepheline crystallization in nuclear waste glass. Int J Appl Ceram Technol. 2008;5(6):666–73.
20. Vienna JD, Kroll JO, Hrma PR, Lang JB, Crum JV. Submixture model to predict nepheline precipitation in waste glasses. Int J Appl Glass Sci. 2017;8(2):143–57.
21. Marcial J, Crum J, Neill O, McCloy J. Nepheline structural and chemical dependence on melt composition. Am Miner. 2016;101(2):266–76.
22. Marcial J, Saleh M, Watson D, Martin SW, Crawford CL, McCloy JS. Boron-speciation and aluminosilicate crystallization in alkali boroaluminosilicate glasses along the $NaAl_{1-x}B_xSiO_4$ and $LiA_{l1-x}B_xSiO_4$ joins. J Non-cryst Solids. 2019;506:58–67.
23. Goel A, McCloy JS, Fox KM, Leslie CJ, Riley BJ, Rodriguez CP, et al. Structural analysis of some sodium and alumina rich high-level nuclear waste glasses. J Non-cryst Solids. 2012;358(3):674–9.
24. Fox K, Edwards T. Refinement of the nepheline discriminator: results of a phase II study. Savannah River National Laboratory, Aiken, SC; 2008. Report No.: SRNS-STI-2008-00099.
25. Fox KM, Newell JD, Edwards TB, Best DR, Reamer IA, Workman RJ. Refinement of the nepheline discriminator: results of a phase I study. Savannah River National Laboratory, Aiken, SC; 2007. Report No.: WSRC-STI-2007-00659.
26. Deshkar A, Ahmadzadeh M, Scrimshire A, Han E, Bingham PA, Guillen D, et al. Crystallization behavior of iron- and boron-containing nepheline ($Na_2O{\cdot}Al_2O_3{\cdot}2SiO_2$) based model high-level nuclear waste glasses. J Am Ceram Soc. 2019;102(3):1101–21.
27. Ahmadzadeh M, Marcial J, McCloy J. Crystallization of iron-containing sodium aluminosilicate glasses in the $NaAlSiO_4$-$NaFeSiO_4$ join. J Geophys Res Solid Earth. 2017;122(4):2504–24.
28. Shaharyar Y, Cheng JY, Han E, Maron A, Weaver J, Marcial J, et al. Elucidating the effect of iron speciation (Fe^{2+}/Fe^{3+}) on crystallization kinetics of sodium aluminosilicate glasses. J Am Ceram Soc. 2016;99(7):2306–15.
29. Utlak SA, Besmann TM. Thermodynamic assessment of the pseudoternary Na_2O–Al_2O_3–SiO_2 system. J Am Ceram Soc. 2018;101(2):928–48.
30. Spear KE, Besmann TM, Beahm EC. Thermochemical modeling of glass: application to high-level nuclear waste glass. MRS Bull. 1999;24(4):37–44.
31. Besmann TM, Spear KE, Beahm EC. Assessment of nepheline precipitation in nuclear waste glass via thermochemical modeling.

In: Smith RW, Shoesmith DW, editors. Proceedings of MRS. Pittsburgh, PA: Materials Research Society, 2000; p. 715–20.
32. Besmann TM, Spear KE. Thermochemical modeling of oxide glasses. J Amer Ceram Soc. 2002;85(12):2887–94.
33. Besmann TM, Kulkarni NS, Spear KE, Vienna JD, Allendorf MD. Modified associate species approach to phase equilibria prediction for oxide glass systems. In: Li H, Ray CS, Strachan DM, Weber R, Yue Y, editors. Ceramic transactions, Westerville, OH: American Ceramic Society, 2005; p. 81–9.
34. Chartrand P, Pelton AD. Modeling the charge compensation effect in silica-rich Na_2O-K_2O-Al_2O_3-SiO_2 melts. Calphad. 1999;23(2):219–30.
35. Pelton AD, Wu P. Thermodynamic modeling in glass-forming melts. J Non-Cryst Solids. 1999;253(1):178–91.
36. Pelton AD, Blander M. Thermodynamic analysis of ordered liquid solutions by a modified quasichemical approach—application to silicate slags. Metallurg Trans B. 1986;17(4):805–15.
37. Li H, Jones B, Hrma P, Vienna JD. Compositional effects on liquidus temperature of Hanford simulated high-level waste glasses precipitating nepheline ($NaAlSiO_4$). In: Peeler DK, Marra JC, editors. Ceramic transactions. Westerville, OH: American Ceramic Society, 1998; p. 279–88.
38. Li H, Su Y, Vienna JD, Hrma P. Raman spectroscopic study – effects of B_2O_3, Na_2O, and SiO_2 on nepheline ($NaAlSiO_4$) crystallization in simulated high level waste glasses. In: Chandler GT, Feng X, editors. Ceramic transactions. Westerville, OH: American Ceramic Society, 2000; p. 469–77.
39. Stanfill BA, Piepel GF, Vienna JD, Cooley SK. Nonlinear logistic regression mixture experiment modeling for binary data using dimensionally reduced components. Qual Reliabil Eng Int. 2020;36(1):33–49.
40. Kroll JO, Vienna JD, Nelson ZJ, Skidmore CH. Results from phase 5 study on nepheline formation in high-level waste glasses containing high concentrations of alumina. Richland, WA: Pacific Northwest National Laboratory; 2018. Report No.: PNNL-27555.
41. Lonergan CE, Kroll JO, Skidmore CH, Nelson ZJ. X-ray diffraction and product consistency test results for the phase 6 study of nepheline formation in hanford high-level waste glasses. Richland, WA: Pacific Northwest National Laboratory; 2019. Report No.: PNNL-29023.
42. Piepel GF, Stanfill BA, Cooley SK, Jones B, Kroll JO, Vienna JD. Developing a space-filling mixture experiment design when the components are subject to linear and nonlinear constraints. Quality Eng. 2019;31(3):463–72.
43. Pedregosa F, Varoquaux G, Gramfort A, Michel V, Thirion B, Grisel O, et al. Scikit-learn: machine Learning in Python. J Mach Learn Res. 2011;12:2825–30.

SUPPORTING INFORMATION

Additional supporting information may be found online in the Supporting Information section.

How to cite this article: Sargin I, Lonergan CE, Vienna JD, McCloy JS, Beckman SP. A data-driven approach for predicting nepheline crystallization in high-level waste glasses. *J Am Ceram Soc*. 2020;103:4913–4924. https://doi.org/10.1111/jace.17122